**Li-Farn Yang**
Associate Professor.
Mem. ASME
Department of Mechanical Engineering,
National Chung Cheng University,
Taiwan, R.O.C.

**Meng-Sang Chew**
Associate Professor.
Mem. ASME
Department of Mechanical Engineering
and Mechanics,
Lehigh University,
Bethlehem, Pennsylvania 18015

**Jer-Nan Juang**
Principal Scientist.
Fellow AIAA
Spacecraft Dynamics Branch,
NASA Langley Research Center,
Hampton, Virginia 23681

# Concurrent Mechanism and Control Design for the Slewing of Flexible Space Structures

*An integrated single-step design approach to the synthesis of a mechanical device and an active controller is presented for slew maneuvers of flexible space structures. A mechanical device consists of a noncircular gear pair that acts as a varying gear ratio transmission between an electro-mechanical actuator and a flexible structure. Such a system has been introduced as an analytical application in minimizing flexural vibrations in the slewing maneuver of flexible space structures such as large solar panels and satellites in space. Only a simple regulator-type feedback controller is called for to control this complex electro-mechanical-and-structural system and the purpose is to design this complex system in an integrated procedure to achieve low flexural vibrations of the structure. Numerical simulations of the slewing control tasks for a planar articulated double-beam structure are presented.*

## 1 Introduction

Interest in orbiting very large space structures has resulted in the need to maneuver and control flexible structures. This need is driving research into an integrated approach that incorporates mechanism synthesis and system control design so that the maneuvering characteristics of large flexible space structures may be improved. Several large flexible space structures such as the Mobile Satellite, the Large Deployable Reflector, and the Freedom Space Station form the basis for much of present research into the control of flexible space structures.

In a slewing maneuver of a flexible structure driven by an actuator under regulator feedback control, the structural dynamic behavior has been extensively investigated [1-7]. In Refs. 1-4, 6, and 7, the regulator control law has been used for the driving actuator due to the simplicity of such a choice. However, the resulting flexural vibrations of the flexible structure are tunable only through the feedback gains, and are therefore not entirely satisfactory. Direct actuating control on the flexural vibrations on the other hand will not result in a simple regulator-type feedback controller and results in a very complex control implementation such as adaptive control. To compensate for the structural flexibility in response to external disturbance while enhancing the reliability, the concept of adaptive structures [8, 9] has been adopted and applied to space construction. However, very sophisticated sensory and control techniques are needed in conjunction with the smart structures to carry out their designated missions.

It may be noted that much of current research in control theory has been approached from the perspective that the mechanical-structural subsystem is a given, and a controller is then synthesized to accomplish some given objective. On the other hand, the mechanical and structural engineers have looked at the mechanical-structural design as the final design goal and have left the control issues to the control engineers who come after them. Such sequential design procedures, though, result in "optimal" subsystems within the respective disciplines, and do not result in a reliable, efficient, or cost effective system. As such, the resulting system can be improved if the mechanical and the control design processes are integrated. With such a philosophy, it is then possible to enable trade-offs in complexities between the mechanical-structural aspects of the system with that of the controller.

The objective of this article is to integrate the mechanical and control aspects of the design along with a structural system such that a simple and more robust regulator-type feedback controller may be used. It can be anticipated that in this process the mechanical subsystem would become a little more complex.

Many questions arise out of such an approach. First, it needs to be determined if the increase in complexity in the mechanical subsystem will result in a greater reduction in the complexity of the control system. Secondly, there is the question of whether it is indeed possible to bring about such interdisciplinary design in an integrated manner. Finally, the performance of the new modified system needs to be shown to be superior to that of the system based on the classical approach.

## 2 Description of System

The problem of suppressing the flexural vibrations of flexible structures has inspired the introduction of a simple mechanical

Contributed by the Mechanisms Committee and presented at the Mechanisms Conference, Phoenix, AZ, Sept. 13-16, 1992, of THE AMERICAN SOCIETY OF MECHANICAL ENGINEERS. Manuscript received Sept. 1992; revised April 1993. Associate Technical Editor: G. L. Kinzel.

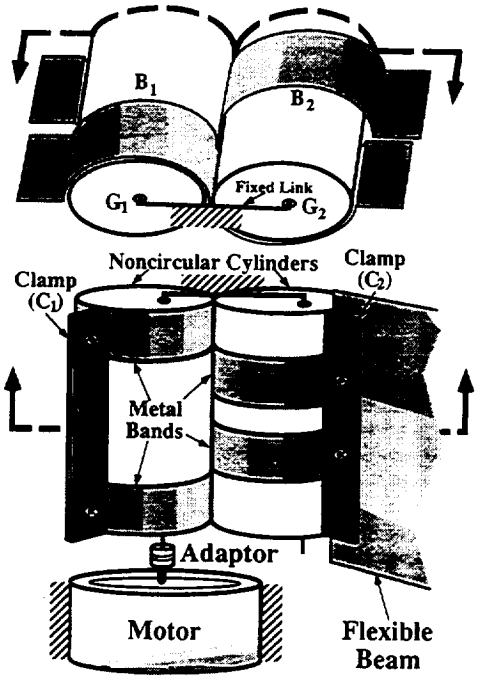


Fig. 1 A pair of noncircular gears wrapped via thin bands

device in conjunction with control law, for tuning the slewing characteristics of a flexible structure for minimum flexural vibrations. An investigation into its applicability and its concurrent design is the subject that will be developed in this article.

Several gearing devices such as gear trains and harmonic devices have been used in transmitting the actuator torques for maneuvering flexible structures [10–16]. All these transmission devices essentially exhibit constant gear ratios during a given operation. This is because circular gears always result in nonvarying gear ratios between the input and output shafts of the transmission because of the constant mechanical advantage.

Based on a given desired maneuvering schedule, it is conceivable that varying gear ratio may help in improving the performance of a slew maneuver. By using such a varying gear ratio, the characteristics inherent to regulator-type controllers at the start of a maneuver can be tuned in such a way that the high initial input torque needed can be reduced. Moreover, the resulting output angular velocity can be regulated in such a way as to reduce the high initial rate-of-change that sets off undesirable vibrations. The slewing maneuver of a flexible articulated double-beam structure is investigated by incorporating noncircular gears to perform this positioning control task. These noncircular gears are installed at the junction between the motor and the flexible structure. Slewing control task of this flexible structure will be modelled and simulated, and the flexural vibrations reduced by simultaneously taking into account the profile of the noncircular cylinders as well as output feedback control law, at the design stage. We shall begin with a brief description on noncircular gear design to serve as background.

**2.1 Mechanical Device: Noncircular Gearing [17].** Many of the existing articles on noncircular gearing [10–16] emphasized design for producing cyclically varying angular velocity, or for generating precise nonlinear functions from a mechanisms viewpoint. A concurrent approach that incorporates the design of such a device in conjunction with feedback control has not been attempted. Moreover, the incorporation of a noncircular mechanical element permits the simplification of the control implementation and it is this objective that forms

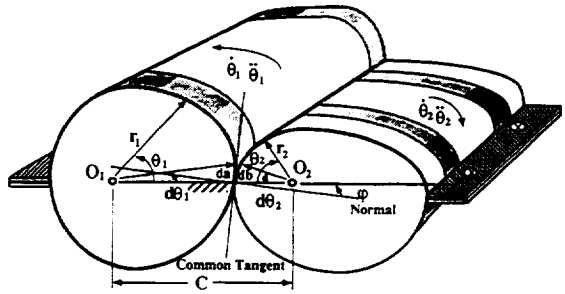


Fig. 2 Configuration of noncircular gears

the basis of this investigation. Figure 1 shows the configuration of a pair of noncircular gears driven by a motor to rotate a flexible beam. Such a noncircular gearing device consists of:

(*1*) a pair of noncircular cylinders ($\mathbf{G}_1$, $\mathbf{G}_2$,),
(*2*) two pairs of thin metal bands ($\mathbf{B}_1$, $\mathbf{B}_2$),
(*3*) two pairs of clamps ($\mathbf{C}_1$, $\mathbf{C}_2$), and
(*4*) a fixed arm to hold the two cylinders at a constant distance apart.

The system features a pair of noncircular cylinders, around which two pairs of thin metal bands wrap. These two specially designed cylinders $\mathbf{G}_1$ and $\mathbf{G}_2$ with noncircular profiles, meshed through the use of two pairs of thin metal bands $\mathbf{B}_1$ and $\mathbf{B}_2$ as shown in Fig. 1. The two noncircular cylinders are wrapped in opposite directions, and are then tightly clamped by two clamps $\mathbf{C}_1$ and $\mathbf{C}_2$ at the two ends of the metal bands. When the profiles of the two noncircular cylinders are properly designed, pure rolling contact exists between the two cylinders. A fixed arm, which is grounded, is used to hold the two cylinders together such that the center distance always remains constant. The varying gear ratio due to the noncircular profiles produces varying output-to-input speeds. This speed variation tunes the kinematic characteristics of the flexible space structures during rapid slewing maneuvers while being controlled by a regulator-type feedback controller. Pure rolling contact, and hence low friction between the noncircular cylinders, reduces stiction nonlinearities to the system. The shear force, normally taken by the gear teeth, is taken by the tension in the bands ($\mathbf{B}_1$ and $\mathbf{B}_2$).

Figure 2 shows the cross section of the noncircular gears. Two noncircular gears $O_1$ and $O_2$ that are kept apart at a constant center distance $\overline{O_1O_2} = C$ have the instantaneous pitch radii denoted by $r_1$ and $r_2$, respectively. Assume that gears $O_1$ and $O_2$ are the driving and the driven gears, respectively, with the corresponding input and output angles, $\theta_1$ and $\theta_2$. The synthesis of their profiles is presented in Appendix I. The pitch curves of the two noncircular cylinders are given by Eqs. (I.2) and (I.3) in the Appendix. To simplify the specification of the varying gear ratio, a hyperbolic gear ratio function is used and is defined as [10–15]:

$$N_g(\theta_2) = \frac{\dot{\theta}_2}{\dot{\theta}_1} = \frac{c_2}{c_1 + \theta_2} \tag{1}$$

where $c_1$ and $c_2$ indicate two parameters which can be determined by providing two end points on the hyperbolic gear ratio function. As an example, the pitch curves of the noncircular cylinders based on the hyperbolic function given by Eq. (1) above, is shown in Fig. 3(*a*) for the range of 0 deg–90 deg of output rotation, and is plotted in Fig. 3(*b*). The synthesis process towards arriving at the pitch curves for a hyperbolic gear ratio function as shown in Fig. 3 will be discussed below.

During the slewing control process, the noncircular gears characterized by a hyperbolic gear ratio function given by Eq. (1) will transform the output angular displacement and velocity to behave in such a way that the flexural vibrations are suppressed. The hyperbolic function in Fig. 3(*a*) may be specified

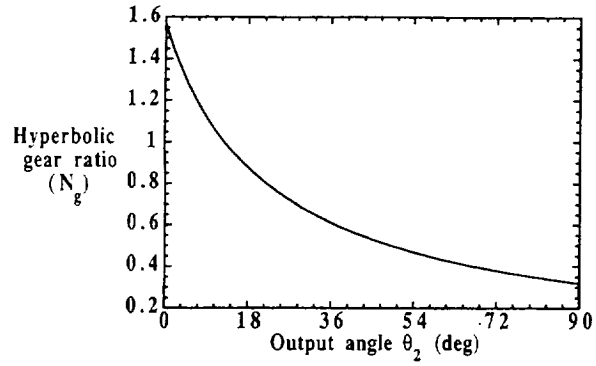


Fig. 3(*a*) Hyperbolic gear ratio as a function of driven gear rotation angle

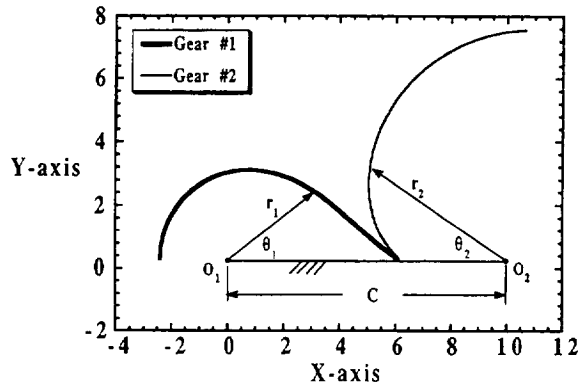


Fig. 3(*b*) Profiles of noncircular gears with a hyperbolic gear ratio

with the following initial parameter values: $c_1 = \pi/10$, $c^2 = \pi/5$, and $C = 10$. The pitch radii of the two noncircular cylinders can then be found from Eq. (I.2):

$$r_1 = \frac{C\,N_g(\theta_2)}{1+N_g(\theta_2)}, \quad r_2 = \frac{C}{1+N_g(\theta_2)} \tag{2}$$

From Eq. (I.3), the input angle $\theta_1$ of the driving cylinder can be computed:

$$\theta_1 = \frac{1}{c_2}\left[c_1\theta_2 + \frac{\theta_2^2}{2}\right] \tag{3}$$

Plots of the instantaneous pitch radii $r_1$ ($\theta_1$) and $r_2$ ($\theta_2$) in polar coordinates directly confirm whether the requirements of convexity are adhered to. Based on the hyperbolic gear ratio function shown in Fig. 3(*a*), the pitch curves of the two noncircular cylinders are determined and shown in Fig. 3(*b*). The convexities of the two pitch curves confirms the feasibility of the hyperbolic gear ratio function for generating the profiles of these noncircular cylinders.

**2.2 Actuator Dynamics.** The actuator shown in Fig. 1 is directly connected to one of the noncircular gears. A step-down gear box may be built-in into the actuator to proportionally magnify the varying noncircular gear ratio if so needed. The motor may be modelled by a standard armature circuit which is governed by the following differential equation:

$$J_m\ddot{\theta}_1 + \left(C_v + \frac{K_t K_b}{R_a}\right)\dot{\theta}_1 + \tau_a = \frac{K_t}{R_a}e_a \tag{4}$$

where $J_m$ denotes the motor inertia; $C_v$ the viscous drag coefficient; $K_t$ the motor torque constant; $K_b$ the back-emf constant; $R_a$ the armature resistance; $\theta_1$ the output motor angle; $e_a$ the applied voltage for the armature; and $\tau_a$ the available torque from the motor shaft. The available torque $\tau_a$ in Eq. (4) is then transformed to the driving torque $\tau_s$ through a step-down constant gear ratio $N_p$, as well as the varying gear ratio $N_g$ of the noncircular gears so that:

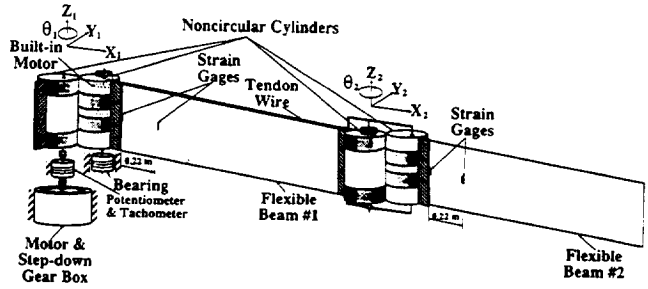


Fig. 4 Configuration of a planar flexible double-beam

$$\tau_a = N_g N_p \tau_s \tag{5}$$

where $\tau_s$ is the input torque to the flexible-link structure. Since the gear ratio in Eq. (I.2) is varying, the input-output relationship between the driving and driven cylinders is governed by a nonlinear transformation which can be shown to be:

$$\begin{bmatrix}\dot{\theta}_1\\ \ddot{\theta}_1\end{bmatrix} = \begin{bmatrix}\dfrac{1}{N_g(\theta_2)} & 0\\ -\dfrac{\dot{N}_g(\theta_2)}{N_g^2(\theta_2)} & \dfrac{1}{N_g(\theta_2)}\end{bmatrix}\begin{bmatrix}\dot{\theta}_2\\ \ddot{\theta}_2\end{bmatrix} \tag{6}$$

Substituting Eqs. (5) and (6) into Eq. (4), the output torque $\tau_s$ to the structure is obtained and is expressed by:

$$\tau_s = \frac{K_t e_a}{R_a N_g N_p} - \frac{C_v + \dfrac{K_t K_b}{R_a}}{(N_g N_p)^2}\dot{\theta}_2 + \frac{J_m}{(N_g N_p)^3}\left[N_g N_p \ddot{\theta}_2 - N_p \dot{N}_g \dot{\theta}_2\right] \tag{7}$$

where the time rate-of-change of the gear ratio $\dot{N}_g$ in Eq. (7) can be computed from:

$$\dot{N}_g = \left[\frac{dN_g}{d\theta_2}\right]\dot{\theta}_2 \tag{8}$$

The input voltage across the actuator $e_a$ in Eq. (7), is generated according to the active feedback controller and the varying noncircular gear ratio $N_g$, for driving the flexible beam and for suppressing the flexural vibrations.

## 3 Dynamics of Flexible Systems Incorporating Noncircular Gearing and Actuators

In this article, the dynamics of a planar articulated double-beam structure, in conjunction with cylinder-type noncircular gears will be investigated. A description of the closed-loop regulation control system will also be described in Section 3.2.

**3.1 Planar Flexible Articulated Double-Beam.** In this subsection, a derivation of the dynamic equation is presented for a planar flexible double-beam of which the outer flexible beam (#2) is articulated at the tip of the inner beam (#1) to result in a flexible articulated double-beam structure as shown in Fig. 4. The actuation for the two beams is accomplished in a way that the first (inner) beam is driven by a motor via a built-in gear train, while the second (outer) beam is manipulated by another motor through a wire or tendon configuration (see Fig. 4). Moreover, the second motor is built-in and concatenated axially to the output noncircular cylinder of the first beam. These two flexible beams are modeled as the cantilever beams of the same length $L$ along the $x$-axis. Flexural vibrations are permitted during the slewing motion of the arms. We begin by expanding the deflection of the flexible beams in modal form.

Dynamic modeling of different flexible spacecrafts has been conducted in [2, 7, 20–23] to implement the specific control missions such as the slewing maneuver, deployment, and retrieval. Note that while there may be other methods for beam modeling [20–23] the modal representation is deemed to be sufficiently accurate and is very efficient for the purpose of this investigation. Lagrange's method [18, 19] is now applied to derive the dynamic equations of motion as follows. In Fig. 4, denote $\theta_{b_1}$ as the root angle of the first flexible beam and $\theta_{b_2}$ as the root angle of the second beam, measured relative to the local coordinates $x_1 - y_1$. Let the state vector $\xi$ be defined as:

$$\xi = [\theta_{b_1}, \theta_{b_2}, q_1^T, q_2^T]^T; \quad \begin{cases} q_1^T = [q_{1_1}, \ldots, q_{1m_1}], \text{ and} \\ q_2^T = [q_{2_1}, \ldots, q_{2m_2}] \end{cases} \tag{9}$$

where $q_{1_i}$ $(i = 1, \ldots, m_1)$ are the general coordinates corresponding to the shape functions $\psi_{1_i}$ for discretization of the bending deflection of the first flexible beam. The quantities $q_{2_i}$ $(i = 1, \ldots, m_2)$ and $\psi_{2_i}$ are similarly defined for the forebeam [3, 4, 7, 19, 22, 23]. Accordingly to Eq. (9), an input vector for the flexible articulated beams can be described by:

$$\tau = [\tau_{s_1}, \tau_{s_2}, \underbrace{0, \ldots, 0}_{m_1+m_2}]^T \tag{10}$$

Assume that the structural damping of the two flexible beams are negligibly small so that it will be excluded from the equations of motion. Then, application of Lagrange's equations of motion [18, 19] to such an articulated structure leads to the following dynamic equations:

$$\mathbf{M}\ddot{\xi} + \mathbf{K}\xi = \tau + f(\xi, \dot{\xi}) \tag{11}$$

where $f(\xi, \dot{\xi})$ represents a nonlinear force vector and is written as:

$$f(\xi, \dot{\xi}) = [f_1, f_2, f_3, f_4]^T; \begin{cases} f_1 = \dfrac{\rho L^3}{2} s\theta_{b_2}\dot{\theta}_{b_2}^2 - Ls\theta_{b_2} h_2^T \dot{q}_2 \dot{\theta}_{b_2} \\ f_2 = -s\theta_{b_2}\psi_1^T(L) h_2^T \dot{q}_1 \dot{q}_2 + Ls\theta_{b_2} h_2^T \dot{q}_2 \dot{\theta}_{b_1} \\ f_3 = -\dfrac{\rho L^2}{2}\psi_1(L) s\theta_{b_2}\dot{\theta}_{b_2}^2 + s\theta_{b_2}\psi_1(L) h_2^T \dot{q}_2 \dot{\theta}_{b_2} \\ f_4 = -Ls\theta_{b_2} h_2 \dot{\theta}_{b_1}\dot{\theta}_{b_2} + h_2 s\theta_{b_2}\psi_1^T(L)\dot{q}_1\dot{\theta}_{b_2} \end{cases} \tag{12}$$

where $h_2 = \int_0^L \rho\psi_2(x_2)dx_2$ and $s\theta_{b_2} = \sin(\theta_{b_2})$. The inertia matrix $\mathbf{M}$ in Eq. (19) becomes:

$$\mathbf{M} = \begin{bmatrix} 4I_1 & \dfrac{1}{2}\rho L^3 c\theta_{b_2} & -\rho L^2\psi_1^T(L) - p_1^T & -Lh_2^T c\theta_{b_2} \\ & I_2 & -\dfrac{1}{2}\rho L^2\psi_1^T(L)c\theta_{b_2} & -p_2^T \\ \textbf{Symmetry} & & \rho\psi_1(L)\psi_1^T(L) + \rho L\hat{\mathbf{I}}_1 & h_2\psi_1^T(L)c\theta_{b_2} \\ & & & \rho L\hat{\mathbf{I}}_2 \end{bmatrix} \tag{13}$$

where $\mathbf{I}_i$ $(i = 1, 2)$ are the moments of inertia of beams #1 (inner beam) and #2 (outer beam), $p_1 = \int_0^L \rho\, x_1[\psi_{1_1}(x_1), \ldots, \psi_{1m_1}(x_1)]^T dx_1$, $p_2 = \int_0^L \rho\, x_2[\psi_{2_1}(x_2), \ldots, \psi_{2m_2}(x_2)]^T dx_2$, and $c\theta_{b_2} = \cos(\theta_{b_2})$. Moreover, $\hat{\mathbf{I}}_1$ and $\hat{\mathbf{I}}_2$ are $m_1 \times m_1$ and $m_2 \times m_2$ identity matrices, respectively. For the flexibility of the double beams, the stiffness matrix is described by

$$\mathbf{K} = \mathbf{Diag}[0, 0, \rho L\omega_1^2, \rho L\omega_2^2]; \quad \begin{cases} \omega_1 = \mathbf{Diag}[\omega_{1_1}, \ldots, \omega_{1m_1}], \text{ and} \\ \omega_2 = \mathbf{Diag}[\omega_{2_1}, \ldots, \omega_{2m_2}] \end{cases} \tag{14}$$

where $\omega_{1_i}$ $(i = 1, \ldots, m_1)$ and $\omega_{2_j}$ $(j = 1, \ldots, m_2)$ are the modal frequencies corresponding to shape functions $\psi_{1_i}(x_1)$ and $\psi_{2_j}(x_2)$, respectively.

As for the actuator dynamics, two idler gear boxes (with constant gear ratios $N_{p_i}$) $(i = 1, 2)$ and two pairs of noncircular gears (with varying gear ratios $N_{g_i}$) are utilized for the torque transmission of the two beams. From Eq. (7), the applied beam torques $\tau_{s_1}$ and $\tau_{s_2}$ in Eq. (10) can be replaced by:

$$\tau_{s_i} = \frac{K_{t_i} e_{a_i}}{R_{a_i} N_{g_i} N_{p_i}} - \frac{C_{v_i} + \dfrac{K_{t_i} K_{b_i}}{R_{a_i}}}{(N_{g_i} N_{p_i})^2}\dot{\theta}_{b_i} + \frac{J_{m_i}}{(N_{g_i} N_{p_i})^3}[N_{g_i} N_{p_i}\ddot{\theta}_{b_i} - N_{p_i}\dot{N}_{g_i}\dot{\theta}_{b_i}], \; i = 1, 2 \tag{15}$$

Note that, instead of the conventional motor's back-emf with a constant gear ratio, the back-emf in Eq. (15) can be tuned through the varying gear ratios $N_{g_i}$ $(i = 1, 2)$.

Referring to the sensors, the rotational angle is measured by a ten-turn rotary potentiometer, whereas the angular velocity is calibrated by a tachometer. Strain gages are used to sense the bending moments along two flexible beams. Suppose two strain gages are placed along each flexible beam respectively at positions $x_a$ and $x_b$. An output measurement equation can be written in the following matrix form:

$$\hat{e} = [e_{t_1}, e_{t_2}, e_{p_1}, e_{p_2}, e_{0_1}(x_a), e_{0_1}(x_b), e_{0_2}(x_a), e_{0_2}(x_b)]^T$$
$$= \mathbf{Diag}[c_{t_1}, c_{t_2}, c_{p_1}, c_{p_2}, \mathbf{C}_{\epsilon_1}, \mathbf{C}_{\epsilon_2}][\dot{\theta}_{b_1}, \dot{\theta}_{b_2}, \theta_{b_1}, \theta_{b_2}, \dot{q}_1^T, \dot{q}_2^T]^T$$
$$\mathbf{C}_{\epsilon_i} = c_{s_i} h \begin{bmatrix} \dfrac{\partial^2\psi_{i_1}}{\partial x_1 \partial x_1}(x_a), \ldots, \dfrac{\partial^2\psi_{im_1}}{\partial x_1 \partial x_1}(x_a) \\ \dfrac{\partial^2\psi_{i_1}}{\partial x_2 \partial x_2}(x_b), \ldots, \dfrac{\partial^2\psi_{im_2}}{\partial x_2 \partial x_2}(x_b) \end{bmatrix}, \quad \text{for } i = 1, 2 \tag{16}$$

where $h$ is the half thickness of the flexible beams, and $c_{p_i}$, $c_{t_i}$, $c_{s_i}$ $(i = 1, 2)$ are sensory conversion factors as defined in Ref. 7.

Substituting Eqs. (15) and (16) into Eq. (11) provides:

$$\overline{\mathbf{M}}\ddot{\xi} + \overline{\mathbf{C}}\dot{\xi} + \mathbf{K}\xi = \mathbf{B}E_a(t) + f(\xi, \dot{\xi}) \tag{17}$$

where

$$\overline{\mathbf{M}} = \mathbf{M} + \mathbf{Diag}\left[\frac{J_{m_1}}{(N_{g_1}N_{p_1})^2}, \frac{J_{m_2}}{(N_{g_2}N_{p_2})^2}, \underbrace{0, \ldots, 0}_{m_1+m_2}\right],$$

$$\bar{\mathbf{C}} = \mathbf{Diag}\left[\frac{K_{t_1}K_{b_1}}{R_{a_1}} + C_{v_1} - I_{m_1}\frac{\dot{N}_{g_1}}{N_{g_1}}}{(N_{g_1}N_{p_1})^2}, \frac{\frac{K_{t_2}K_{b_2}}{R_{a_2}} + C_{v_2} - I_{m_2}\frac{\dot{N}_{g_2}}{N_{g_2}}}{(N_{g_2}N_{p_2})^2}, \underbrace{0, \ldots, 0}_{m_1+m_2}\right],$$

$$\mathbf{B} = \begin{bmatrix} \frac{K_{t_1}}{R_{a_1}N_{g_1}N_{p_1}} & 0 \\ 0 & \frac{K_{t_2}}{R_{a_2}N_{g_2}N_{p_2}} \\ \multicolumn{2}{c}{\mathbf{O}_{((m_1+m_2)\times 2)}} \end{bmatrix}, \quad \text{and } E_a(t) = \begin{bmatrix} e_{a_1} \\ e_{a_2} \end{bmatrix}$$

Equation (17) thus demonstrates a closed-loop system of a flexible double-beam structure in conjunction with two pairs of noncircular gears. Note that the time rate-of-change of the gear ratios $N_{g_i}$ ($i = 1, 2$), in damping matrix $\bar{\mathbf{C}}$ of Eq. (17), is given by Eq. (8). Furthermore, such a form as shown in Eq. (17) facilitates the incorporation of output feedback control, which will be the subject of discussion in the next subsection.

**3.2 Regulator Feedback Controller For a Slewing Maneuver.** Regulator feedback controller is a linear optimal control law to perform an asymptotically stable closed-loop system in which each state is driven toward its final state under a controlled process. Such a controller is simple and robust, and is therefore very desirable for implementation into real applications. Slewing maneuvers of the double-beam flexible structure discussed earlier will be implemented. To be able to apply the linear regulation control algorithm, the dynamics described by Eq. (17) have to be linearized by neglecting the nonlinear force vector $f(\xi, \dot{\xi})$. This linearization still results in a stable system as discussed in [3, 4, 7]. Then the linearized dynamic equations can be transformed into a system of first order state equations so that:

$$\dot{\epsilon} = \tilde{\mathbf{A}}\epsilon + \tilde{\mathbf{B}}E_a; \quad \begin{cases} E_a = -\tilde{\mathbf{G}}\hat{e}, & \text{and} \\ \hat{e} = \mathbf{C}_f\epsilon \end{cases} \tag{18}$$

where

$$\epsilon = \begin{bmatrix} \xi \\ \dot{\xi} \end{bmatrix}, \quad \tilde{\mathbf{A}} = \begin{bmatrix} \mathbf{O} & \mathbf{I} \\ -\overline{\mathbf{M}}^{-1}\mathbf{K} & -\overline{\mathbf{M}}^{-1}\overline{\mathbf{C}} \end{bmatrix}, \quad \text{and } \tilde{\mathbf{B}} = \begin{bmatrix} \mathbf{O} \\ \overline{\mathbf{M}}^{-1}\mathbf{B} \end{bmatrix}$$

The output feedback gain matrix $\tilde{\mathbf{G}}$ is determined by the following control analysis. The control criteria for this linear regulation problem is to minimize a quadratic performance index of the form:

$$J = \int_0^\infty [\hat{e}^T\mathbf{Q}\hat{e} + E_a^T\mathbf{R}E_a]dt, \quad \mathbf{Q} \geq 0 \text{ and } \mathbf{R} > 0 \tag{19}$$

The output feedback gains can be determined by:

$$\tilde{\mathbf{G}} = \mathbf{R}^{-1}\tilde{\mathbf{B}}^T\mathbf{P}, \quad \mathbf{P} > 0 \tag{20}$$

where the positive definite matrix $\mathbf{P}$ satisfies the following algebraic Riccati equation:

$$\tilde{\mathbf{A}}^T\mathbf{P} + \mathbf{P}\tilde{\mathbf{A}} + \mathbf{C}_f^T\mathbf{Q}\mathbf{C}_f - \mathbf{P}\tilde{\mathbf{B}}\mathbf{R}^{-1}\tilde{\mathbf{B}}^T\mathbf{P}^T = 0 \tag{21}$$

In general, a successful slewing implementation must fulfill two dynamic aspects: system stability and smooth continuous behavior. The output feedback gain matrix $\tilde{\mathbf{G}}$ given by Eq. (20) will ensure the asymptotical stability of poles in the closed-loop system $[\tilde{\mathbf{A}} - \tilde{\mathbf{B}}\tilde{\mathbf{G}}\mathbf{C}_f]$. As it was discussed in Section 2.1, the cylinder-type noncircular gears are capable of varying the actuating torque to tune the slewing characteristics so that the control effort may be reduced. Hence, the incorporation of the noncircular gears and the feedback controller must be considered together from the perspective of an integrated design process. In other words, in the slewing control of flexible structures the flexural vibrations of the beam are reduced by taking into account the profile design of the noncircular cylinders as well as the output feedback controller gains, concurrently at the design stage. An optimizer is employed to determine not only the pitch curves of the noncircular cylinders, but also the output feedback gains that will minimize the vibrational amplitudes. This incorporation of noncircular gears results in a controller design that is simpler and more robust, for implementing a slew maneuver of flexible links in multibody flexible structures in the hostile space environment. Such an integrated design approach will be presented in the following section.

## 4 Integration of Feedback Controller Design With Noncircular Gear Design

For an integrated mechanism and control design, the Generalized Reduced Gradient (GRG) method [24] is employed to determine the optimal designs of noncircular gear ratios together with control gains for suppressing flexural vibrations in a slew maneuver. This nonlinear programming approach will iterate for a vector of design variables that will extremize a given function, subject to some equality and inequality constraints.

$$\textbf{Minimize:} \quad F(\bar{x}); \quad \bar{x} = [x_1, x_2, x_3, \ldots, x_N]^T \in R^N \tag{22}$$

$$\textbf{Subject to:} \quad \begin{cases} \phi_k(\bar{x}) \geq 0; & k = 1, \ldots, K \\ \Psi_l(\bar{x}) = 0; & l = 1, \ldots, L \end{cases} \tag{23}$$

where

$\bar{x}$ = a column vector of design variables,
$N$ = total number of design variables,
$F(\bar{x})$ = design criteria or objective function,
$\phi_k(\bar{x})$ = $K$ inequality constraint functions,
$\Psi_l(\bar{x})$ = $L$ equality constraint functions.

The hyperbolic parameters for the noncircular gear ratio function along with the regulator control gains are assigned as design variables to be determined by the GRG algorithm. A quadratic cost function is developed for minimizing the modal vibrational amplitudes. The dynamics of the flexible structures may be expressed as a system of first-order state equations. These first-order state equations become the equality constraint functions which must be satisfied in terms of dynamic response as the optimal design variables are being searched. Inequality constraint functions are specified to bound the gear ratios or the control torques. The GRG algorithm then numerically determines the design variables, which consist of the parameters of noncircular gear ratio and the control gains, so that the flexural vibrations of the structures are minimized during the slew maneuver. A close examination of each of the elements necessary for the specification and definition of this problem in the format of the GRG algorithm is given below.

**4.1 Design Variables.** In addition to the parameters for the noncircular gears and control gains, the design variables of this optimization problem will include the states of vibrational modes for the flexible structures. Assume that $n$ multiple structures are connected through $n$ noncircular gear pairs with $m$ flexible modes specified for the vibrational motion of each

structure in a slew maneuver. Then the design variable vector is written as:

$$\bar{x} = [c,\ \mathcal{G},\ \epsilon(k),\ \epsilon(k+1)]^T \tag{24}$$

where $c$ is a $1 \times 2n$ vector of parameters for noncircular gears, $\mathcal{G} = [[\bar{G}(i, j), j = 1, \ldots, 2n(m+1)], i = 1, \ldots, n]$ is a $1 \times 2n(m+1)$ vector of control gains, and $\epsilon(k)$, $\epsilon(k+1)$ at two different times $t = k$, $k+1$ are $1 \times 2n$ state vectors in the first-order state equation at two sequential times. The number of design variables, i.e., $N = 8n + 2m$, is obtained by summing the number of elements in Eq. (24).

**4.2 Cost Function.** Design variables in Eq. (24) will be determined to minimize the cost function which is defined as:

$$F(x) = \sum_{i=1}^{n} \{\bar{\omega}_i[\theta_{b_i}(k) - \theta_{b_i k}]^2 + \bar{\omega}_{i+n}[\dot{\theta}_{b_i}(k) - \dot{\theta}_{b_i k}]^2\} + \sum_{i=1}^{n}\sum_{j=1}^{m} \bar{\omega}_{ij} q_{ij}^2(k) \tag{25}$$

where $\theta_{b_i}(k)$ and $\dot{\theta}_{b_i}(k)$ $(i = 1, 2, \ldots, n)$ are the slewing angles and angular velocities at time $k$; $\theta_{b_i k}$ and $\dot{\theta}_{b_i k}$ are the desired states, and $q_{ij}(k)$ are the magnitudes of the vibrational modes at time $k$. The weighting factor for each slewing state is $\bar{\omega}_i$ $(i = 1, 2, \ldots, 2n)$, and those for the magnitudes of the $j$th vibrational mode of the $i$th structure are denoted by $\bar{\omega}_{ij}$ $(i = 1, 2, \ldots, n;\ j = 1, 2, \ldots, m)$. The cost function attempts to control the slewing states, such as angle and angular velocity, at a given time $k$ to some specified magnitude, while minimizing the amplitudes of vibrational modes of flexible structures.

**4.3 Constraints.** The equality constraint functions are provided by:

$$\Psi_i(\bar{x}) = \epsilon(k+1) - \tilde{\epsilon}(k+1), \quad \text{for} \quad i = 1, \ldots, 2n \tag{26}$$

The state vector $\tilde{\epsilon}$ at time $k+1$ is governed by the discrete-type first-order state equations as follows:

$$\begin{cases} \tilde{\epsilon}(k+1) = \tilde{\mathbf{A}}\epsilon(k) + \tilde{\mathbf{B}}E_a(k) + \tilde{f}; \\ E_a(k) \quad = \tilde{\mathbf{G}}\mathbf{C}_f\epsilon(k) \end{cases}$$

where

$$\tilde{\mathbf{A}} = \begin{bmatrix} \mathbf{0} & \mathbf{I} \\ -\overline{\mathbf{M}}^{-1}\mathbf{K} & -\overline{\mathbf{M}}^{-1}\overline{\mathbf{C}} \end{bmatrix}, \quad \tilde{\mathbf{B}} = \begin{bmatrix} \mathbf{0} \\ \overline{\mathbf{M}}^{-1}\mathbf{B} \end{bmatrix}, \text{ and } \quad \tilde{f} = \begin{bmatrix} \mathbf{0} \\ \overline{\mathbf{M}}^{-1} f(\xi, \dot{\xi}) \end{bmatrix}$$

Equation (26) shows the first-order dynamic equations of multibody flexible structures, which must be satisfied by the feasible design variables. Several inequality constraint functions $\phi_k(\bar{x})$ defined in Eq. (23) are specified to bound the range of each varying gear ratio and torque limitation of each motor.

The analysis described in this section can now be used to bring about an integrated design of the noncircular gears as well as the control gains so as to coordinate the actuating torque during a slewing maneuver, with minimum flexural vibrations. In the following section, three different simulations will be implemented by using different mechanisms or control techniques for stabilizing and tuning 90 deg-slew tasks of a planar double-beam structure via this integrated mechanism and control design approach.

## 5 Simulations of a Flexible Articulated Double-Beam

This section includes simulations of 90 deg-slew maneuvers implemented for a planar flexible double-beam, whose slewing characteristics will be tuned in conjunction with the noncircular gear. The flexural vibration of this double-beam structure is characterized by applying two vibrational modes to each beam.

**Table 1 Model parameters for a flexible articulated double-beam**

a. Beam motors:

| (1)Beam #1 motor: | | (2)Beam #2 motor: | |
|---|---|---|---|
| $K_{t_1} = 0.0346$ | $Nm/Amp$ | $K_{t_2} = 9.3 \times 10^{-3}$ | $Nm/Amp$ |
| $K_{b_1} = 0.0342$ | Volt-sec/rad | $K_{b_2} = 9.2 \times 10^{-3}$ | Volt-sec/rad |
| $R_{a_1} = 4$ | Ohm | $R_{a_2} = 1.1$ | Ohm |
| $I_{m_1} = 4.7 \times 10^{-6}\ kgm^2$ | | $I_{m_2} = 2.3 \times 10^{-6}$ | $kgm^2$ |
| $N_{p_1} = 1$ | | $N_{p_2} = 1$ | |

b. Steel beam:

| | | |
|---|---|---|
| Length | $L = 1.0$ | m |
| Rigidity | $EI = 0.71$ | $Nm^2$ |
| Density | $\rho = 0.47916$ | kg/m |
| Thickness | $h = 0.041 \times 10^{-2}$ | m |

c. Parameters of noncircular gear ratio:

| (1)Beam #1 gears: | (2)Beam #2 gears: |
|---|---|
| $c_{11} = \frac{\pi}{10}$ | $c_{21} = \frac{\pi}{64}$ |
| $c_{12} = \frac{3\pi}{5}$ | $c_{22} = \frac{3\pi}{11}$ |

**Table 2 Weighting and feedback gain matrices for a flexible articulated double-beam**

a. Weighting matrices:

State weighting matrix:

$$\mathbf{Q} = \mathbf{Diag}[\,250\ 100\ 10\ 10\ 10\ 10\ 250\ 100\ 10\ 10\ 10\ 10\,]$$

Input weighting matrix: $\mathbf{R} = [\,500,\ \ 500\,]$

b. Output feedback gain matrix:

$$\tilde{\mathbf{G}} = \begin{bmatrix} -0.7018 & -0.0547 & 0.5633 & 2.4793 & -0.2597 & 1.3766 \\ 0.0864 & -0.4439 & 0.0345 & 4.9427 & -0.2104 & -2.9872 \\ -1.1214 & -0.2117 & 0.8029 & -0.6719 & 0.3141 & 0.0668 \\ -0.0844 & -0.5758 & 0.2477 & -0.3145 & 0.2148 & 0.0165 \end{bmatrix}$$

**Table 3 Optimization problem for noncircular gears and control gain in a flexible articulated double-beam**

Minimise: Eq. (25) with $\varpi_1 = \varpi_{11} = 5500, \varpi_2 = \varpi_{12} = 4500$, and $\varpi_3 = \varpi_4 = 5000$

Design variables:

$$\bar{x} = [\,c_{11},\ c_{12},\ c_{21},\ c_{22},\ \mathcal{G}_{(1\times 24)},\ c(k),\ c(k+1)\,]^T \text{ where}$$
$$\epsilon = [\theta_{b_1}, \theta_{b_2}, q_{11}, q_{12}, q_{21}, q_{22}, \dot{\theta}_{b_1}, \dot{\theta}_{b_2}, \dot{q}_{11}, \dot{q}_{12}, \dot{q}_{21}, \dot{q}_{22}]^T$$

Subject to:

(1) Equality constraint functions: Eq. (26)

(2) Inequality constraint functions:

$$\begin{cases} \phi_1(\bar{x}) = c_{12} - 0.1 \times \left[c_{11} + \frac{10.280244\pi}{180}\right] \geq 0, \\ \phi_2(\bar{x}) = c_{22} - 0.1 \times \left[c_{21} + \frac{3.281172\pi}{180}\right] \geq 0, \\ \phi_3(\bar{x}) = -u_1(k) + 1.5 \geq 0, \quad \phi_4(\bar{x}) = u_1(k) - 0.2 \geq 0, \\ \phi_5(\bar{x}) = -u_2(k) + 1.5 \geq 0, \quad \phi_6(\bar{x}) = u_2(k) - 0.2 \geq 0 \end{cases}$$

Starting point:

$$\bar{x}^0 = [\tfrac{\pi}{10}, \tfrac{3\pi}{5}, \tfrac{\pi}{22}, \tfrac{6\pi}{11}, -0.702, 0.086, -0.055, -0.444, -7.845, 4.965, -132.538, -18.617, -0.193, -17.848, -26.478, -236.05, -1.121, -0.084, -0.212, -0.576, -1.867, 0.219, -1.798, -0.888, 0.588, -3.278, -0.221, -0.218, 0.1812, 0.09078, 0.063, -0.0012, 0.016, 0.000264, 0.2, 0.208, -0.0062, 0.0039, -0.0051, 0.0016, 0.2, 0.208, -0.0064, 0.0039, -0.0049, 0.0015, -0.088, 0.914, -0.281, -0.03, 0.3, -0.071]^T.$$

Bounds on design variables:

(1) Upperbounds:

$$\bar{x}_{max} = [0.3, 1.9, 0.16, 1.73, -0.69, 0.13, -0.08, -0.44, -7.6, 5.1, -132.3, -18.4, -0.08, -17.6, -26.2, -235.8, -1.53, -0.04, -0.36, -0.74, -1.6, 0.4, -1.5, -0.6, 0.7, -3.0, -0.02, -0.01, 24 \times [10]]^T$$

(2) Lowerbounds:

$$\bar{x}_{min} = [0.29, 1.86, 0.12, 1.69, -0.69, 0.13, -0.08, -0.44, -8.0, 4.7, -132.7, -18.8, -0.3, -18.0, -26.6, -236.2, -1.53, -0.04, -0.36, -0.74, -2.0, 0.01, -1.9, -1.0, 0.3, -3.4, -0.4, -0.4, 24 \times [-10]]^T.$$

Three different cases will be considered for comparison. The first case (case 1) is with 1:1 ratio circular gears; the second (case 2), with the noncircular gears associated with a given hyperbolic gear ratio as expressed in Section 2.1; and the third (case 3), with the integration of mechanism and control design.

The parameters of the double-beam system are shown in Table 1. Their weighting matrices and resulting regulator-type control gain matrices derived in Section 3.2 are summarized in Table 2. Moreover, the parameters of the noncircular gear ratio as shown in Eq. (3) are given in Tables 1 for case 2. Based on Eqs. (24) to (26), the problem definition for the optimal design for the 90 deg-slew maneuver of a flexible double-beam structure is summarized in Table 3. The results shown in Figs.

5(*a*)-5(*j*), which are associated with 1:1 circular gears, demonstrate the severe vibrations of the two beams at 0.64 seconds. Therefore, the state vector $\xi$ and time-rate state vector $\dot{\xi}$ at that instant are selected as design variables, in conjunction with the four parameters $c_{11}$, $c_{12}$, $c_{21}$, and $c_{22}$ for two different noncircular gear ratios, and the control gain matrix $\tilde{\mathbf{G}}_{(2\times 12)}$. This give a total of fifty-two design variables for the optimization problem.

The quadratic cost function is constructed so as to suppress vibrational modes of two flexible beams while simultaneously keeping the two slewing angles $\theta_1$, $\theta_2$ at 0.18117 rad and 0.090778 rad, respectively, and two angular velocities $\dot{\theta}_1$, $\dot{\theta}_2$ at 0.19956 rad/sec and 0.20797 rad/sec, respectively, which are related to the severe vibrations at 0.64 seconds [see Figs. 5(*a*)-5(*d*)].

The equality constraint function are provided by twelve first-order state equations $\Psi_i(\bar{x})$ ($i = 1, \ldots, 12$) which must always be satisfied during the optimization process. Two inequality constraint functions $\phi_1(\bar{x})$ and $\phi_2(\bar{x})$ are given to make two gear ratios greater than 0.1. Four other inequality constraint functions $\phi_i(\bar{x})$ ($i = 3, 4, 5, 6$) are specified to bound the two control torques to be between 0.2 and 1.5 Nm.

Based on these initial values of the design variables, the starting value of cost function $F(\bar{x}^0)$ equals 21.772 while the final cost is 0.0157333 at the minimum of $F(\bar{x})$. Accordingly, the optimal solution to the design parameters yields:

$$c_{11\text{opt}} = 0.29,\ c_{12\text{opt}} = 1.9,\ c_{21\text{opt}} = 0.134177,\ c_{22\text{opt}} = 1.69386,$$

and

$$\tilde{\mathbf{G}}_{\text{opt}} = \begin{bmatrix} -0.694 & -0.084 & -7.6 & -132.3 & -0.288 & -26.2 & -1.533 & -0.355 & -1.999 & -1.899 & 0.3 & -0.399 \\ 0.1332 & -0.439 & 4.70607 & -18.799 & -17.875 & -236.191 & -0.043 & -0.741 & 0.01 & -0.606 & -3.4 & -0.399 \end{bmatrix} \quad (27)$$

Three simulation results for such a 90 deg-slew maneuver are summarized and are characterized by lines #1, #2, and #3 in Figs. 5(*a*)-5(*j*). The results with the 1:1 circular gears are indicated by a thin solid line #1, the results for the general noncircular gears by a dashed line #2, and the results for the integrated mechanism and control design by a thick solid line #3. Two flexible steel beams slew through 90.0 degrees in 8.0 seconds as shown in Figs. 5(*a*) and 5(*b*), respectively. Note that the noncircular gears for optimal integrated design slow down the beam slewing during the first 5-degrees of rotation, thereby providing a smoother actuation to the desired final angle than that in the presence of the circular gears.

In Figs. 5(*c*) and 5(*d*), the three results show that the beam angular velocities damp out in approximately 8.0 seconds. The higher frequency modes are clearly present in the results using circular gears but are nearly vanishing in the other two results for noncircular gears (lines #2 and #3). That indicates the efficient suppression of structural vibration in the presence of noncircular gears, in particular, the case subjected to optimal integrated design (line #3). Also the slewing angular velocity (lines #2 and #3) in the presence of noncircular gears is shown to be smoother after 1.0 seconds which implies that the beam slewing and vibrational motion have been tuned through the use of the noncircular gears. Moreover, the peak magnitude of the angular velocity is also significantly reduced through this integrated design approach.

Figures 5(*e*) and 5(*f*) show the two control torques for beam #1 and beam #2, respectively. The optimal integrated design reduces the amplitudes of the first and second modes associated with beam #1 by 21 percent compared to the unoptimized noncircular gears (line #2) in Figs. 5(*g*) and 5(*i*). However, compared to the results associated with the circular gears in Figs. 5(*g*) and 5(*i*), the amplitudes of the first and second modes for beam #1 are reduced by some 64 percent. In Figs. 5(*h*) and 5(*j*), the reduction of the amplitudes of beam #2 for the first and second modes is about 38 percent when comparing the results for the general noncircular gears (line #2). The reduction is as high as 52 percent, when compared to the results associated with the circular gears (line #1). As a result, the peak amplitude of each mode as illustrated in Figs. 5(*g*)-5(*j*) is considerably reduced, particularly, based on the optimal integrated design approach.

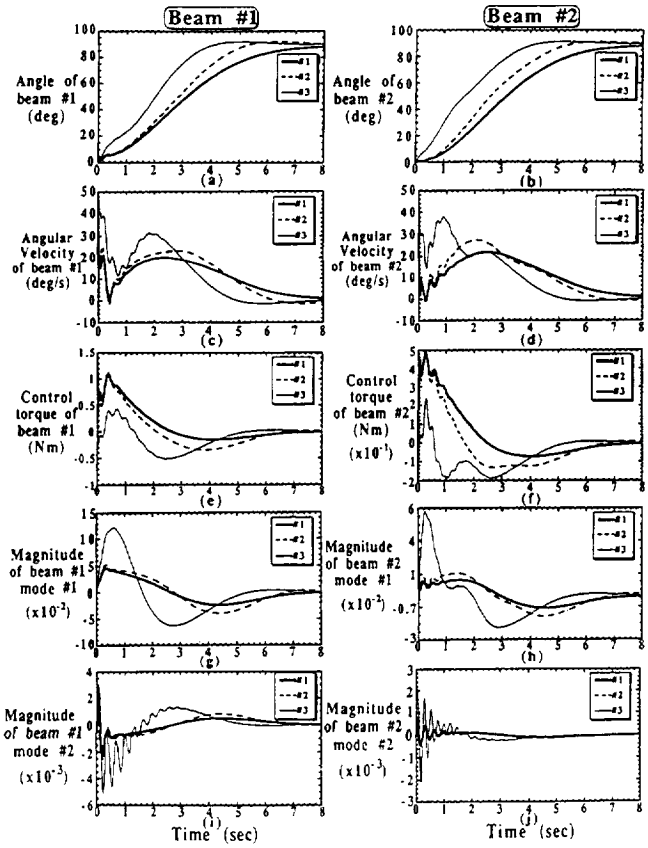


**Fig. 5 Simulation results of a planar flexible double-beam for a 90 deg-slew maneuver**

## 6 Conclusion

Rapid and large slew-angle maneuvers almost always result in severe flexural vibration that can barely subside within a short period of time if not properly taken care of. An investigation of a novel integrated mechanism and control approach has been conducted for tuning the slewing characteristics of the flexible space structures such that the flexural vibrations can be considerably suppressed through the incorporation of a nonlinear mechanical element. The compromise between mechanism parameters and control law is accomplished through the use of optimization, for the sense of concurrent design. A pair of noncircular gears have been designed to generate the varying-ratio transmission for the slewing maneuvers of a planar articulated double-beam structure. Such a noncircular gear pair characterizes a pair of wrapped cylinders whose profiles have been synthesized to comply with the convexity criterion in conjunction with a given parametric function of the hyperbolic gear ratio. Then, an electro-mechanical-structural system is constructed in an integrated fashion along with a nonlinear transmission between the actuators and the space structures. The slewing responses have been shown to be tuned well, and the flexural vibrations are effectively suppressed by

means of this concurrent mechanism and control design approach. These simulation results indicate the crucial role of integrating mechanism and control in the design procedure for slewing maneuvers of flexible structures.

A comparison of the simulation results with the noncircular gears and the circular gears implies that the hyperbolic gear ratio has been useful and practical for tuning slewing maneuvers and suppressing flexural vibrational motions so as to enhance system performances. Therefore, this synthesis scheme paves the way for integrating mechanisms design with control for rapid and large-angle slew maneuvers of the flexible space structures.

## Acknowledgments

The first and second authors wish to acknowledge NASA Grant No. NAG1-830 from the Spacecraft Dynamics Branch at NASA Langley Research Center, Hampton, VA, for supporting this research as well as U.S. Patent No. 5,146,803 [17].

## References

1 Dubowsky, S., and Gardner, T. N., 1975, "Dynamic Interactions of Link Elasticity and Clearance Connections in Planar Mechanical Systems," ASME *Journal of Engineering for Industry*, May, pp. 652-661.

2 Dwyer, T. A. W., III, and Batten, A. L., 1985, "Exact Multiaxial Spacecraft Attitude Maneuvers With Torque Saturation," *Proc. of IEEE International Conference on Robotics and Automation*, St. Louis, Missouri, March, pp. 978-983.

3 Juang, J.-N., Horta, L. G., and Robertshaw, H. H., 1986, "A Slewing Control Experiments for Flexible Structures," *Journal of Guidance, Control and Dynamics*, Vol. 9, Sept.-Oct., pp. 599-607.

4 Ghaemmaghami, P., and Juang, J.-N., 1987, "A Controller Design for Multibody Large Angle Maneuvers," *Proc. of International Symposium on the Mathematics of Networks and Systems*, Phoenix, Arizona, June 15-19.

5 Fujii, H., and Ishijima, S., 1987, "The Mission Function Control for Deployment and Retrieval of Subsatellite," *Proc. of the Guidance, Navigation and Control Conference*, AIAA Paper No. 87-2326, Aug.

6 Junkins, J. L., Rahman, Z., Bang, H., and Hecht, N., 1989, "Near-Minimum-Time Maneuvers of Flexible Vehicles: A Lyapunov Design Method," *Proc. of the 7th VPISU Symposium on Dynamics and Control of Large Structures*, VPI, Blacksburg, VA, May 8-10.

7 Juang, J.-N., Yang, L.-F., Huang, J.-K., and Macauley, R., 1989, "Rapid Rotational/Translational Maneuvering Experiments of a Flexible Steel Beam," *1989 American Control Conference*, Pittsburgh, PA, June 21-23.

8 Wada, B. K., Fanson, J., and Crawley, E., 1990, "Adaptive Structures," *Journal of Intelligent Material Systems and Structures*, Vol. 1, No. 2, April, pp. 157-174.

9 Wada, B. K., 1990, "Adaptive Structures: An Overview," *Journal of Spacecraft and Rockets*, Vol. 27, No. 3, May-June, pp. 330-337.

10 Peyrebrune, H. E., 1953, "Application and Design of Noncircular Gears," *Transactions of the First Conference on Mechanisms*, Purdue University, pp. 21-24.

11 Benford, B. F., 1968, "Customized Motions from Economical 'Almost Standard' Eccentric Gears," *Machine Design*, Sept. 26, pp. 151-154.

12 Cunningham, F. W., 1958, "Noncircular Gears," *Transactions of the Fifth Conference on Mechanism*, Purdue University, pp. 96-103.

13 Bloomfield, B., 1967, "Noncircular Gears," *Gear Design and Application*, McGraw-Hill Book Co., pp. 158-165.

14 Rappaport, S., 1967, "Elliptical Gears for Cyclic Speed Variations," *Gear Design and Applications*, McGraw-Hill Book Co., pp. 166-168.

15 Miano, S. V., 1967, "Twin Eccentric Gears," *Gear Design and Applications*, McGraw-Hill Book Co., pp. 169-173.

16 Freudenstein, F., and Chen, C.-K., 1991, "Variable-Ratio Chain Drives With Noncircular Sprockets and Minimum Slack-Theory and Application," ASME JOURNAL OF MECHANICAL DESIGN, Vol. 113, Sept., pp. 253-262.

17 U.S. Patent No. 5,146,803, "Noncircular Rolling Joints for Vibrational Reduction in Slewing Maneuvers," Sept. 15, 1992.

18 Greenwood, D. T., 1988, *Principles of Dynamics*, Prentice-Hall, Inc., Englewood Cliffs, NJ.

19 Meirovitch, L., 1971, *Analytical Methods in Vibrations*, Third Printing, MacMillan Company, New York, NY.

20 Book, W. J., 1975, "Feedback Control of Two Beam Joint Systems With Distributed Flexibility," ASME *Journal of Dynamic Systems, Measurement, and Control*, Dec., pp. 424-431.

21 Book, W. J., 1979, "Analysis of Massless Elastic Chains With Servo-Controlled Joints," ASME *Journal of Dynamic Systems, Measurement, and Control*, Vol. 101, Sept., pp. 187-192.

22 Rakhsha, F., and Goldenberg, A. A., 1985, "Dynamic Modeling of a Single-Link Flexible Robot," *IEEE Trans. on Automatic Control*, pp. 984-989.

23 Hastings, G. G., and Book, W. J., 1986, "Verification of a Linear Dynamic Model for Flexible Robotic Manipulators," *IEEE Trans. on Automatic Control*, pp. 1024-1029.

24 Gabriele, G. A., 1975, "Application of the Reduced Gradient Method to Optimal Engineering Design," M.S. Thesis, School of Mechanical Engineering, Purdue University, Dec.

# APPENDIX I

## Noncircular Gearing Synthesis

The profiles of a pair of noncircular cylinders as shown in Fig. 1 can be developed using the following gearing synthesis. Figure 2 shows the cross section of two noncircular gears centered at $O_1$ and $O_2$ with the pitch radii $r_1$ and $r_2$, respectively. Their angular displacements are indicated by $\theta_1$ and $\theta_2$, angular velocities $\dot{\theta}_1$ and $\dot{\theta}_2$, and angular acceleration $\ddot{\theta}_1$ and $\ddot{\theta}_2$, respectively. The center distance $\overline{O_1O_2}$ is denoted by $C$ and the pressure angle by $\phi$. The necessary condition for rolling contact between two gears $O_1$ and $O_2$ as shown in Fig. 2 is that the equivalent tracking arc length must satisfy: $da = db \Rightarrow r_1 d\theta_1 = r_2 d\theta_2$. Suppose that the varying gear ratio $N_g(\theta_2)$ is defined as the ratio of the output to input angular velocities, then:

$$N_g(\theta_2) = \frac{\dot{\theta}_2}{\dot{\theta}_1} = \frac{r_1}{r_2} \text{ where } r_1 + r_2 = C \tag{I.1}$$

The pitch radii $r_1$ and $r_2$ of the two noncircular cylinders can be shown to be:

$$r_1 = \frac{CN_g(\theta_2)}{1 + N_g(\theta_2)}, \quad r_2 = \frac{C}{1 + N_g(\theta_2)} \tag{I.2}$$

The input angle $\theta_1$ of the driving cylinder $O_1$ can be computed by integrating Eq. (I.1) as given by:

$$\theta_1 = \int_0^{\theta_2} \left[ \frac{1}{N_g(\theta_2)} \right] d\theta_2 \tag{I.3}$$